# Investigation of water vapour sorption mechanism of starch-based pharmaceutical excipients

Article (Accepted Version)

# Investigation of water vapour sorption mechanism of starch-based pharmaceutical excipients

Saeid Rajabnezhad[a], Taravat Ghafourian[a], Ali Rajabi-Siahboomi[b], Shahrzad Missaghi[b], Majid Naderi[c], Jonathan P. Salvage[d], Ali Nokhodchi[a,*]

[a] Pharmaceutics Research Laboratory, Arundel Building, School of Life Sciences, University of Sussex, BN1 9QJ, Brighton, UK; [b]Colorcon, Inc., Global Headquarters, 275 Ruth Road, Harleysville, PA 19438, USA; [c]Surface measurement Systems, Unit 5, Wharfside, Rosemont Road, Alperton, London. HA0 4PE; [d]School of Pharmacy and Biomolecular Sciences, Huxley Building, University of Brighton, Brighton, BN2 4GJ, UK;

*** Corresponding Author: Ali Nokhodchi (a.nokhodchi@sussex.ac.uk; tel; +441273872811)**

**Abstract**

Starch-based excipients are commonly used in oral solid dosage forms. The effect of particle size and pregelatinisation level of starch-based excipients on their water absorption behaviour have been evaluated. The results showed that starch-based excipients have type ii isotherms, indicating that the principal mechanism of sorption is the formation of monolayer coverage and multilayer water molecules (10-80 RH%). It was found that the particle size of starch-based excipients did not have any influence on the rate of water sorption, whereas the level of pregelatinisation changed the kinetics of water sorption-desorption. Results showed that the higher the degree of pregelatinisation, the higher the rate of water absorption irrespective of particle size. SEM images showed that a partially gelatinised starch had a firm granular structure with small pores and channels on the surface while a fully gelatinised starch had more irregular and spongy like surface with a degree of fractured particles.

**Keywords:** Starch powder, pre-gelatinisation, DVS, Starch 1500, water sorption-desorption, BET theory

## 1. Introduction

Presence of water in pharmaceutical solid powders has always been a challenge in the formulation development of solid dosage forms, as it may have a detrimental effect on the physical and chemical stability of active pharmaceutical ingredients (APIs) and excipients in the formulation of oral solid dosage forms (Malamataris, Goidas, & Dimitriou, 1991; Nokhodchi, Ford, & Rubinstein, 1997). The interaction of water with solid surfaces could occur via van der Waals forces, hydrogen bonding or ion-dipole force (Reutzel-Edens, Braun, & Newman, 2018). After interaction of water with surface of solid powder, the moisture or water either becomes (i) physisorbed to the surface (monolayer water formation), (ii) chemisorbed (multilayer water formation), (iii) disordered adsorption on regions of a solid surface which is similar to the monolayer formation, (iv) water inclusion as a result of physical entrapment of water to the solid surface or (v) formation of hydrates (Likar, Taylor, Fagerness, Hiyama, & Robins, 1993; Reutzel-Edens et al., 2018). Presence of water not only modifies the pharmaceutical and mechanical properties of the finished product but may also reduce the physicochemical stability and eventually the pharmacological activity of the drugs as well. As moisture is freely available in the atmospheric environment during the processing, manufacture, packaging and storage of the solid dosage forms, it is significantly important to understand the mechanism by which water interacts with powder blend with respect to its behaviour at various relative humidity (RH) levels. To understand the effect of RH on the extent of water-solid interaction, several factors such as hygroscopicity of the powder, physical and chemical structure of the material, presence and availability of OH groups, powder density and porosity as well as particle size must be considered (Malamataris *et al*., 1991). The structure of starch and cellulose excipients are highly influenced by hydrogen bonding between water molecules and water-solid molecules (Delwiche, Pitt, & Norris, 1991). Depending on the state of

water when interacting with pharmaceutical solids, physicochemical and pharmaceutical properties of the powder blend may vary (Malamataris, Goidas, & Dimitriou, 1991; Nokhodchi, Ford, & Rubinstein, 1997). To understand water-solid interactions, it is pivotal to understand how different particle size fractions of powder affect water adsorption /absorption and desorption.

Moisture sorption isotherms are one of the most promising methods in describing the relationship between RH and water activity ($a_w$) of the samples at a constant temperature, by setting out a correlation between equilibrium moisture content (EMC) at a constant temperature and water activity (Staudt *et al*, 2013). Unlike food sciences, water activity is an important concept, the effects of which have not yet been thoroughly evaluated in pharmaceutics and pharmaceutical technology. Water activity ($a_w$) is defined as a thermodynamic activity of the available water associated with a solid powder. It is also defined as a fugacity of water associated with the solid powder to the fugacity of pure water to escape into the surrounding environment (Cundell, 2015; Ostrowska-Ligęza, Jakubczyk, Górska, Wirkowska, & Bryś, 2014; Reutzel-Edens et al., 2018). For the construction of sorption isotherms, two cycles of sorption and desorption form a loop (hysteresis). Usually, not all the sorbed water molecules are able to dissociate once associated with solid powders. Hysteresis could be regarded as a fingerprint for every single powder under study. The shape of the hysteresis loop and the position where the gap starts and ends is a unique feature for any particular powder when analysing the absorption and desorption of water molecules from a solid surface. As mentioned above, the hysteresis indicates that some water molecules always remain within the powder when it is subjected to the desorption process at the same equilibrium relative humidity (ERH) level (Kawongolo, 2013). Hysteresis occurs due to the conformational structure change that appears when starch-based excipients are exposed to different humidity

102 levels. When starch hydrates, it swells and owing to physical shrinkage and conformational change
103 in the structure of the hydrated starch molecules, the entrapped water molecules cannot be easily
104 dissociated (hysteresis in the sorbed/desorbed profile). It means that the entrapped absorbed water
105 molecules (hydrogen atoms of the available OH groups of starch bonded to the oxygen atom of
106 the absorbed/ adsorbed water molecule) can no longer dissociate. Hysteresis could also indicate
107 that the solid materials are either mesoporous (2-50 nm) or macroporous (>50 nm) (Saripella,
108 Mallipeddi, & Neau, 2014b).
109
110 It has been found that even though the pores on starch-based particles are large enough to
111 accommodate water molecules, the opening of the pores could be immensely narrow to allow any
112 water molecules to penetrate into the pores. This is known as the ink bottle phenomenon, which
113 resembles the narrow-mouthed bottles (Saripella, Mallipeddi, & Neau, 2014b). According to this
114 model, adsorption of moisture to the ink-bottled shape pores takes place when the first layer of
115 water molecules is adsorbed onto the walls and the neck of the pores and cavities. Condensation
116 of the water molecules occurs initially on the neck of the pore at a lower water activity ($a_w$) of 0.1
117 (ink bottle). When the neck is filled with water molecules but can no longer sorb any water
118 molecules, the pores may act as a closed pore. Therefore, the mechanism of absorption in the ink-
119 bottle is similar to the closed-end pore (when the pores are filled with water molecules). Following
120 further increase in the water pressure and activity ($a_w$) more water molecules build up on the wall
121 of the pores and cavities. It continues until the gas-like core becomes too small to attract the water
122 layers of the opposite surface to allow additional condensation to occur. This is how water sorption
123 takes place. On the other hand, when desorption initiates from the filled ink-bottle pores and
124 cavities, removal of the already condensed water molecules from the filled pores are delayed

compared with the pores of similar sizes. Uniform, but not complete removal of water molecules occurs in the desorption stage and it continues as long as the mechanical stretching of the desorption phase is sufficient enough to take out another water molecule. It implies the presence of the hysteresis gap during the desorption phase. However, if it continues and the water molecules in the cavity are overstretched as a result of desorption cycle, cavitation within the pores would result which may cause steep drop during the desorption cycle by a further reduction in water activity ($a_w$). The full hysteresis shows the complete mechanism of sorption-desorption cycles from porous solid materials with varying pores and cavities sizes (Zeng *et al*., 2014).

It is also important to note that the water molecules initially taken up into the pores behave as freezable water having the bulk water properties (Saripella, Mallipeddi, & Neau, 2014a). This phenomenon occurs at low water activity ($a_w$) levels which are when monolayer formation takes place. By increasing the vapour pressure or activity ($a_w$) which is translated into ERH when the value is multiplied by 100, multilayer coverage starts to build up on the wall of the pores until the pseudo-gas core becomes low enough to induce further condensation to occur (Zeng *et al*., 2014). Another explanation for the existence of hysteresis, especially for starch-based excipients is that starch is prone to swelling upon absorbing water molecules (Saripella, Mallipeddi, & Neau, 2014 b), leading way to its disintegration properties. Among the explanations given in this paper, some other possibilities can explain the existence of hysteresis, including enthalpy and entropy effects, physical change in conformation of starch powder due to the entry of water ((Malamataris, Goidas, & Dimitriou, 1991; Nokhodchi, Ford, & Rubinstein, 1997).

To quantify the relationship between the equilibrium moisture content and the states of water interaction with powders, several empirical, semi-empirical and theoretical mathematical models

and equations have been developed and used by many researchers (Anderson, 1946; Brunaubr & Emmett, 1935; Brunauer, Emmett, & Teller, 1938; Iglesias & Chirife, 1995; Young & Nelson, 1967a; Young & Nelson, 1967b; Peleg, 1988, 1993; Staudt et al., 2013; Yu & Li, 2015). Amongst all these models and theories, Young and Nelson's model composed of series of equations is the favourable model for starch-based excipients (Young & Nelson, 1967a; Young & Nelson, 1967b; Malamataris et al., 1991; York, 1981) which describes the mechanism of water sorption. According to this model, water associated with pharmaceutical solids could either be monolayer, multilayer and internally absorbed (bulk) water. In other words, Young and Nelson model can estimate the bulk water molecules through measuring the desorbed water (Saripella *et al*., 2014b). Various modified starches are available in the market, where the native starch grains are partially or fully gelatinized through chemical or physical/mechanical methods. Starch 1500® is a partially gelatinized product using physical/mechanical methods. This hydromechanically modified native corn (maize) starch contains two main polymers; amylose (AM) and amylopectin (AMP). Starch 1500 is one of the most widely used starch-based excipients in pharmaceutical oral solid dosage forms with various functional benefits such as being used as a diluent, disintegrant, moisture scavenger and stability enhancer.

This study investigates the interaction of moisture (water molecules) with Starch 1500 to understand the intrinsic effect of water associated with Starch 1500 as well as an approximation of the rate of atmospheric water interaction when the powder is exposed to different relative humidities. The behaviour of water absorption by different particle size fractions of Starch 1500 (<45 µm, 45-125 µm and >125 µm) was manifested. In addition, the effect of pre-gelatinisation degree of corn starch on the sorption and desorption behaviour of water molecules was also

evaluated. In this study, Lycatab-PGS was used as a fully gelatinised starch for comparison. The findings of the current research can help formulation scientists understand the role of water in the formulations containing starch-based excipients.

## 1. Materials and methods

### 1.1.Materials

Starch 1500 (ST 1500), a partially pre-gelatinised (maize) starch NF, Ph Eur, was provided by Colorcon Ltd. (Dartford, UK). Lycatab-PGS (fully gelatinized starch, LPGS) was obtained from Roquette (**Lestrem**, France).

### 1.2.Methods

#### *1.2.1. Particle size separation*

Mechanical sieving was used to separate different particle size fractions of Starch 1500 and Lycatab-PGS. The powders were mechanically shaken for 120 min by 90-degree vibrational oscillation to obtain particle size fractions of <45, 45-125 μm and >125 μm. Powders retained on the selected sieves were collected for further analysis, such as measurement of particle size distribution and determination of span value.

#### *1.2.2. Particle size distribution and analysis*

In order to check to see if the mechanical sieving has separated the particles efficiently, the resulting particle size fractions were tested by laser diffraction particle size analyser (Sympatec, Germany) connected to HELOS/RODOS with a lens capable of measuring particle size up to 875 μm. Approximately 1-2 g of each sample was placed into the funnel of the VIBRI and powder was

transferred into the equipment to measure the particle size. The closest channel was found by initial measurement and the lens was selected according to the size distribution pattern. The size analysis was carried out by Windox software (Sympatec, Germany).

### *1.2.3. Powder sizing*

Span value is an additional parameter showing the range of the particle size distribution of the powder. Span shows volume-based size distribution, which indicates how far apart $D_{10\%}$ and $D_{90\%}$ points are, normalised with the midpoint ($D_{50\%}$). It is calculated as follows:

$$Span = \frac{D_{90\%} - D_{10\%}}{D_{50\%}} \qquad \text{Equation 1}$$

Therefore, it is the most applied format of expressing the particle size distribution width as a function of median particle size for the particles on cumulative size distribution.

### *1.2.4. Scanning Electron Microscopy (SEM)*

Samples of starch powders were mounted on 12.5 mm diameter specimen stubs using 12 mm carbon adhesive tabs (Agar Scientific, UK) and sputter-coated with 4 nm of platinum using a Quorum Technologies Q150T sputter coater. The samples were imaged on a Zeiss Sigma field emission gun scanning electron microscope; FEG-SEM (Carl Zeiss Microscopy GmbH, Germany) using an Everhart-Thornley secondary electron detector, operating at 5 kV accelerating voltage with a 30 µm aperture and about 8.5 mm working distance.

### *1.2.5. Fourier Transform Infrared Spectroscopy study (FT-IR)*

All the spectra were recorded using the PerkinElmer, UK (UATR attached to the single bounce ATR accessory with a diamond crystal). A small amount of sample was poured over the crystal in order to cover the surface and the pressure gauge was set to the optimum level to minimise the background noise. The background was subtracted with air (no sample). 32 scans were used per sample and the data were recorded with the resolution of 4 $cm^{-1}$.

### *1.2.6. Powder X-ray diffraction (PXRD) study*

Wide-angle X-ray diffraction (Siemens, Germany) was used to analyse the solid-state of the two starch-based excipients (amorphous or crystalline). The PXRD was operated at 40 kV and 40 mA with Cu Kα 209 radiation (λ) at 0.15405 nm. Data were collected at 2θ at the scanning range of 5° to 50° at step intervals of 0.02°.

### *1.2.7. Thermogravimetric analysis (TGA)*

TA Q500 instrument (Waters, UK) was used to analyse the thermogravimetric measure of the samples. Approximately 9-10 mg of the samples equilibrated in different RH% conditions were heated from room temperatures to 495 °C. The peaks were recorded and further analysis, such as derivative of the peaks, was performed on the data using the Pyris software.

### *1.2.8. Water sorption isotherms - dynamic vapour sorption (DVS) method*

Water sorption analyses were performed using the DVS Advantage (Surface Measurement System; UK) automated moisture sorption instrument at 25 ºC. A small amount of each powder sample (13 – 32 mg) was placed onto a clean pan which was attached to a micro-balance. The samples were initially dried for 600 minutes under a continuous flow of air to establish the dry

mass. The samples were then exposed to the following typical partial pressure increase profile: 0 - 90% RH in 10% increments followed by 5% increments to 95% RH. The partial pressure was then decreased in a similar manner for the desorption cycle. Data on mass change were acquired every 5 seconds. At each RH step, the ratio of mass variation over time (dm/dt) was set to 0.002 %/min. This criterion permits the DVS software to automatically determine when equilibrium is reached and a relative humidity step completed. Maximum stage time of 360 minutes and a minimum stage time of 10 minutes were selected for this experiment.

### *1.2.9. Young and Nelson model fit*

Various series of the equations are presented to calculate essential parameters of the Young and Nelson model via point to point analysis using an automated DVS instrument. The model describes a series of equations as shown below (Young & Nelson, 1967a; Young & Nelson, 1967b):

$$\theta = \frac{RH}{RH + (1 - RH) - E} \qquad \text{Equation 2}$$

According to equation 2, $\theta$ is the surface fraction of the powder covered with monolayer water. *RH* stands for relative humidity and the parameter *E* is a variable, which is specific to every material. The value of *E* (equation 3) is determined as described below:

$$E = \exp\left\{\frac{-(q_1 - q_L)}{K_B T_e}\right\} \qquad \text{Equation 3}$$

*Where* $q_1$ and $q_L$ are the heat of water adsorption on the solid powder and heat of condensation of water molecules, respectively, expressed as $Jmol^{-1}$. *KB* is the Boltzman constant ($1.38 \times 10^{-23}$ $JK^{-1}$) and *Te* (*K*) is the experimental temperature. To calculate the surface fraction of the sample covered by water having two or more water molecules thickness ($\psi$), equation 4 is used:

$$\psi = RH(\theta) \quad \text{Equation 4}$$

In order to quantify the fraction of externally absorbed water on the surface of the powder, equation 5 is used, where $B$ is the fraction of the total quantity of water present in multilayer.

$$\beta = -\frac{E(RH)}{E-(E-1)RH} + \frac{E^2}{E-1}\log_e \frac{E-(E-1)RH}{E} - (E-1)\log_e(1-RH) \quad \text{Equation 5}$$

And the final moisture sorption and desorption could be calculated using equations 6 and 7, as shown below:

$$M_s = A(\theta+\beta) + B\psi \quad \text{Equation 6}$$

$$M_d = A(\theta+\beta) + B\theta(RH_{\max}) \quad \text{Equation 7}$$

Where $M_s$ and $M_d$ are the total moisture content of the samples for the sorption and desorption cycles, respectively. $RH$ is the relative humidity and $RH_{max}$ is the maximum target (experimental) set at 95% RH. The total amount of water molecules that the solid holds are the sum of the net amount of internally and externally adsorbed water.

$$A = \frac{\rho_w V_{abs}}{W_m} \quad \text{Equation 8}$$

$$B = \frac{\rho_w V_{ads}}{W_m} \quad \text{Equation 9}$$

The parameters $A$ and $B$ are used to calculate the volume of absorbed, $V_{abs}$ $cm^3$, and adsorbed $V_{ads}$ $cm^3$, water, respectively. $\rho_w$ is the density of water (g $cm^{-1}$) and $W_m$ is the mass of dry sample in (g). $A\theta$ is the fraction of monolayer coverage, $A\ (\theta + \beta)$ is the amount of externally adsorbed water and $B\psi$ is the fraction of internally absorbed water. Iterations of the multiple nonlinear regression method can be used to find the best fit for the experimental data by changing the value of $E$ parameter to obtain the best correlation coefficient.

### *1.2.10. Data analysis*

Data analyses were performed using SPSS 24.0 (SPSS Inc., Chicago, USA) and Minitab 18.0 (Pennsylvania, USA). The data were the mean of triplicate runs ± SD. Student t-test and multiple comparison one-way ANOVA using the Tukey test were used. The data were considered significantly different where $P<0.05$. Linear and nonlinear regression analysis were also performed to fit the observed data with the mathematical models.

## 2. Results and discussion

The particle size fractions of powder samples obtained after mechanical sieving were analysed to calculate particle size distribution and measurement of the span value using laser diffraction particle size analyser. The particle size distribution results are summarised in Table 1 demonstrates the data obtained after mechanical sieving are the specified particle size range (in case of fibrous or needle-shaped particles and very small particles usually mechanical sieving could be erroneous). The results reported in Table 1 indicate that mechanical sieving is a promising method for particle size separation of starch-based excipients.

**Table 1.** Particle size distribution of Starch 1500 and LPGS after mechanical sieving measured by laser diffraction particle size analyser

| **Samples** | $X_{10\%}$ **(µm)** | $X_{50\%}$ **(µm)** | $X_{90\%}$ **(µm)** | ***VMD*** **(µm)** | **Span** |
|---|---|---|---|---|---|
| **Starch 1500 <45 µm** | 8.95 | 20.13 | 42.92 | 23.32 | 1.69 |
| **Starch 1500 45-125 µm** | 28.18 | 56.61 | 80.53 | 55.29 | 0.93 |
| **Starch 1500 >125 µm** | 80.62 | 136.75 | 201.93 | 138.94 | 0.89 |
| **LPGS** | 23.83 | 60.09 | 89.90 | 58.47 | 1.10 |

In terms of the size distribution width, <45 µm of ST 1500 has a wider and broader size distribution pattern compared to a size fraction of 45-125 µm, indicating the possibility of agglomeration due to high surface area and the particulate charge of size fraction <45 µm. On the other hand, Starch 1500 particles having >125 µm particle size do have the least width. This indicates that larger particles are more uniformly distributed in the selected particle size fraction compared to the other two fractions. However, widening of the span value of LPGS particle could be due to the wide particle size distribution of the powder sample, since it was not fractioned, and it was measured as received.

Sorption isotherm and hysteresis of different fractions of ST 1500 compared to LPGS are shown in Figure 1. The shape of the isotherms is used in the interpretation of the mechanism of sorption-desorption, as well as the performance of the sorption process (Inglezakis, Poulopoulos, & Kazemian, 2018). Brunauer and his team (Brunauer, Deming, Deming, & Teller, 1940) classified the sorption isotherms into five different types (types i-v). However, the modern IUPAC method of isotherm classification defines the type vi isotherm (Figure 2), not included in the original Brunauer classification.

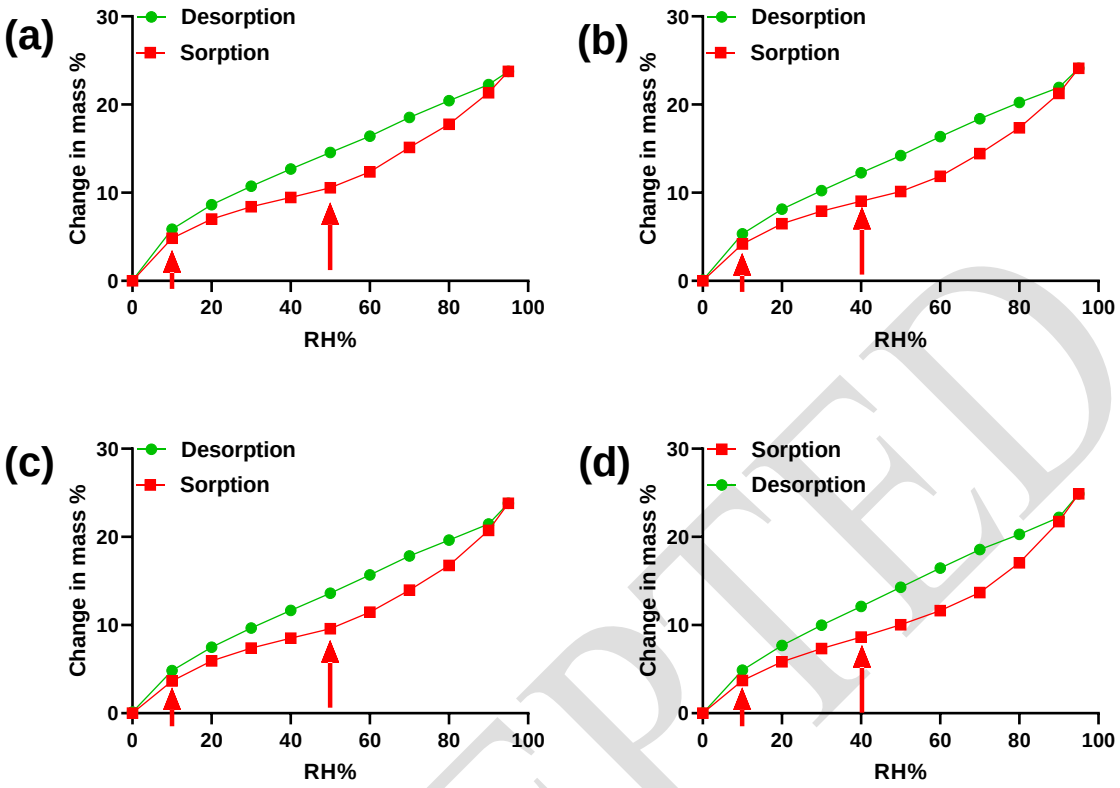


Figure 1. Moisture sorption isotherm and hysteresis; the gap between the two distinct cycles of sorption (red line) and desorption (green line) of (a) ST1500 <45 µm, (b) ST1500 45-125 µm, (c) ST1500 >125 µm and (d) LPGS samples, showing the mass change% with respect to maximum 95% RH level.

According to this classification, it is seen that the specific parts of types ii and iii are similar in shape to types iv and v isotherms, respectively, but overall they exhibit different adsorption patterns. In case of type iii isotherm, the monolayer formation on the microporous adsorbent is stronger than type iv isotherm, as monolayer formation is not limited to the early stage of water adsorption in type iii isotherm (see shapes of type iii and iv isotherms in Figure 2), and this monolayer moisture adsorption can be extended to around 60-70 RH% (Sing, 1994). For types ii and iii as well as types iv and v, sorption of water molecules associated with the surface of the

solid increases as the RH% or $a_w$ increases. This effect is more pronounced for type ii isotherms. Type iii and type iv isotherms require wider water activity level for completion of the formation of monolayer coverage, but this is not the case for type iv and v, as they reach the highest adsorption below the maximum water activity level showing a plateau towards the end (Brunauer *et al*., 1940). In type ii isotherms, monolayer and multilayer physisorption are predominant. This indicates that filling of the pores and open cavities occur at lower ERH levels, whereas the interparticle capillary condensation requires higher water activity (Sing, 1994). Nevertheless, from the sorption isotherms of starch samples (Figure 1), it is evident that starch has a type (ii) shape which is also known as S shape or sigmoidal isotherm with two fundamental deflection points shown by arrows in Figure 1, a characteristic of type ii class.

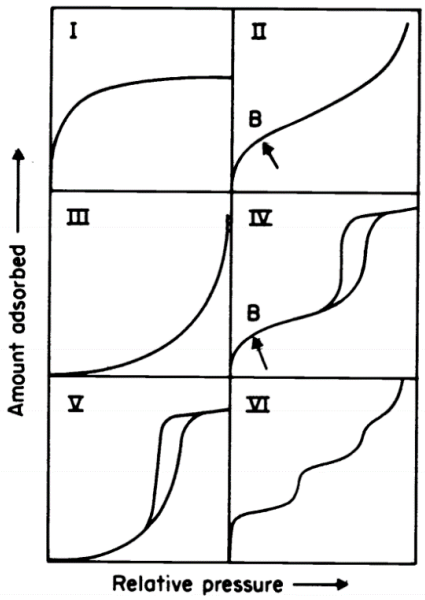


**Figure 2.** IUPAC system of classification of moisture sorption isotherms (Adapted from *Sing*, 1985). Point B indicates the end of the monolayer adsorption and initiation of the formation of multilayer coverage.

The DVS method was applied at 25°C for different fractions of ST 1500 to investigate the effect of particle size on sorption - desorption behaviour of this excipient (Figure 3). The results were

then compared with LPGS to understand the effect of gelatinisation degree on water interactions properties. Moreover, in order to show the effect of particle size and the degree of pre-gelatinisation, change in mass (%) of different fractions of ST 1500 was compared with LPGS (Figure 3.).

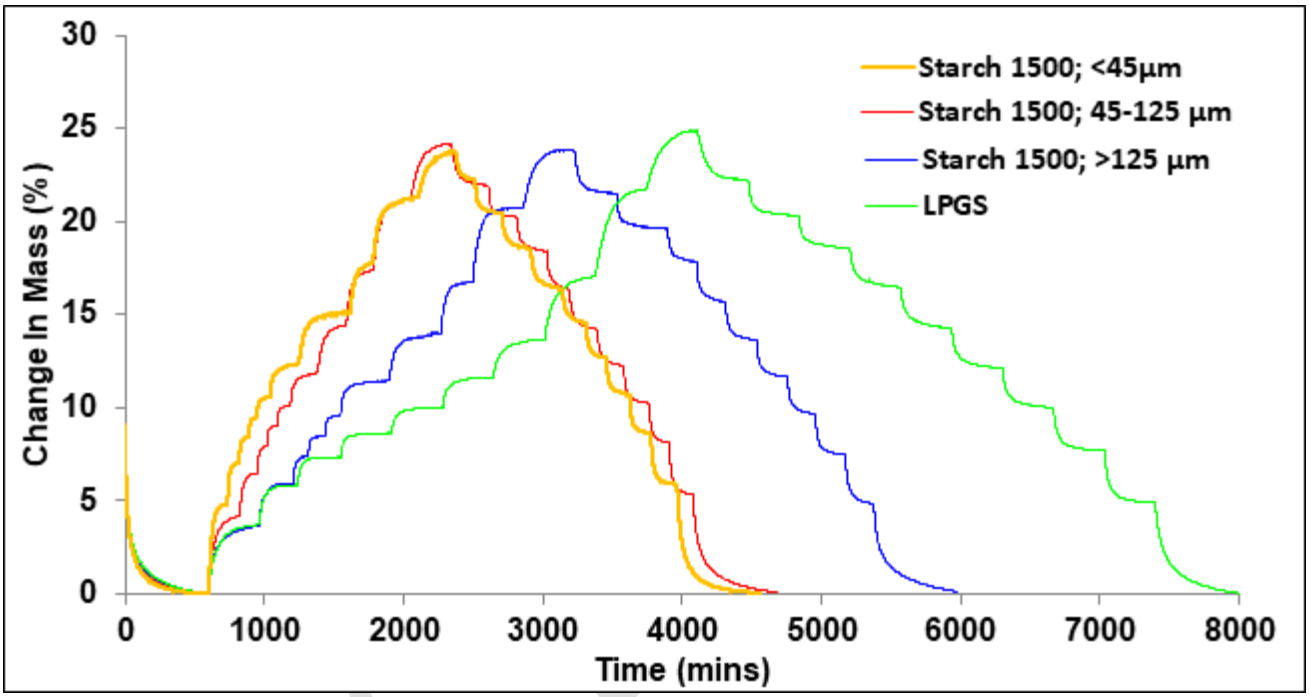


**Figure 3.** Comparison of change in % mass for different fractions of Starch 1500 and LPGS using DVS.

The sorption isotherms for starch-based materials in Figure 1 suggest that the principal mechanism of sorption and desorption is followed by the formation of monolayer coverage and multilayer built up in a wide range of water activity levels; 10-80 RH% (Sing, 1994). According to the data presented in Figures 1 and 3, it is concluded that the shape of the isotherms and the hysteresis of the four samples follow a unique pattern that could be deformed as a characteristic of starch-based excipients. On the other hand, pregelatinisation degree does not seem to influence the net amount of (mass change %) water sorption - desorption pattern of the evaluated starch-based excipients,

or at least it is not a key parameter in water sorption mechanism. If all four isotherms are plotted on the same graph, they almost overlap with each other. It is evident that even though the shape, pattern and the type of isotherms of the starch-based excipients are similar, by increasing the degree of pregelatinisation, LPGS sample requires a longer time to sorb water molecules as a function of % mass change (Figure 3). According to Figure 1, particle size does not influence the kinetics of water sorption for starch-based excipients. On the other hand, by changing the degree of pregelatinisation from partially to fully pregelatinised starch, the rate at which the powders absorb water from the surrounding environment increases.

As shown in Table 1, the span values of the particle fractions of < 45 μm and 45-125 μm are 1.69 and 0.93, respectively. The value is lower (0.39) for >125 μm fraction of ST 1500. Besides showing the dispersity in width for the particles, an increase in span value indicates that smaller particles gain a similar amount of the sorbed water at a shorter period of time and hence approaching the equilibrium condition at a faster rate. This statement does not seem to hold for the effect of particle size. Thus, a change in particle size does not affect the rate of moisture sorption. For instance, if particle size change and the variation in span values solely affect water sorption kinetics, then LPGS sample, which has the span value of 1.10 should gain the moisture in a much slower time than 2000 minutes, which is not the case. Therefore, the degree of pre-gelatinisation appears to govern the rate of moisture sorption. For samples of higher pre-gelatinisation level, it takes longer to uptake the surrounding water and reach the equilibrium state. One-way ANOVA test was performed followed by Tukey hypothetical testing to confirm the significant differences in span values of the samples ($P$<0.05). According to Figure 3, it is observed that the partially pregelatinised samples (ST 1500) have a lower rate of water sorption in terms of the time taken to

reach the maximum water/moisture absorption level, as compared to the fully pregelatinised (LPGS) sample.

The calculated parameters of the Young and Nelson mathematical model are presented in Table 2. The accommodation of the water molecules on the solid surface could be concluded from the *A* and *B* parameters that seem to be constant and identical for all particle sizes of ST 1500 and LPGS with a subtle difference. This means that the volume of absorbed water for ST 1500 samples and LPGS are identical. It further confirms the discussion on the effect of pregelatinisation degree that governs the kinetics of water sorption and is in agreement with the data presented in Figure 3.

**Table 2.** Young and Nelson model parameters calculated for different fractions of Starch 1500 and LPGS

| Parameters | ST 1500 <45 µm | ST 1500 45-125 µm | ST 1500 >125 µm | LPGS |
|---|---|---|---|---|
| ***E*** | 0.094 | 0.126 | 0.156 | 0.174 |
| ***A* (Mol/g)** | 0.002 | 0.002 | 0.002 | 0.002 |
| ***B* (Mol/g)** | 0.004 | 0.005 | 0.005 | 0.005 |
| $R^2$ | 0.996 | 0.996 | 0.997 | 0.996 |

For better understanding, the values obtained from the construction of the sorption isotherms were fitted into the BET model as shown below:

$$M = \frac{M_0 C a_w}{[(1-a_w)(1+(C-1)a_w)]} \qquad \text{Equation 10}$$

where $M$ is the equilibrium moisture content- dry basis (g water/100 g solid), $a_w$ is the water activity, $M_0$ is the monolayer water coverage (g water/ 100 g solid), $C$ and $K$ are the coefficients of sorption parameters of the models to characterise the sorption properties of the solid (Blahovec

& Yanniotis, 2008; Staudt *et al*., 2013; Yu & Li, 2015). Table 3 shows that the smaller particles relatively have higher *C* value (BET model constant, related to the enthalpy of adsorption) which is translated as the affinity of the water molecules to interact with the solid surface. $V_m$ value (monolayer coverage) which is the volume of adsorbed water on the surface of the samples was also calculated and reported in Table 3. Measurement of the surface area of the samples supports the idea that in addition to surface pores and channels, particle size and surface-active sites impacts sorption and desorption of water molecules.

**Table 3**. Calculated parameters ($V_m$ and C) of different fractions of Starch 1500 and its comparison with LPGS sample according to the BET model

| Parameters | ST 1500 <45 µm | ST 1500 45-125 µm | ST 1500 >125 µm | LPGS |
|---|---|---|---|---|
| **Volume Mean particle diameter** | 23.32 | 55.29 | 138.94 | 58.47 |
| **$V_m$ ($cm^3/g$)** | 84.06 | 83.9 | 80.86 | 79.14 |
| ***C*** | 17.14 | 12.31 | 9.69 | 10.34 |
| **Surface area ($m^2/g$)*** | 0.34 | 0.092 | 0.033 | 0.15 |
| **$R^2$** | 99.69 | 99.45 | 99.32 | 99.70 |

*this value is extracted from the laser size analyser on the basis of the true density of the materials

Water binding capacity and water holding power of fully pregelatinised starch (LPGS) might be more than Starch 1500, as a result of the difference in the degree of pregelatinisation, although it appears not to impact the volume of the fractions of the water molecules adsorbed on the surface of the samples. On the other hand, as discussed earlier, pregelatinisation degree lowers the rate of water sorption when comparing partially and fully pregelatinised starch excipients (Figure 3). Also, higher $V_m$ value indicates the ability of more water molecules being adsorbed on the surface

418 of the powder. Therefore, by reducing the surface area the volume of the absorbed water is also
419 reduced.
420 For a stronger conclusion, surface morphology, pores and channels were investigated using SEM
421 imaging. ST 1500 (Figure 4 (A)) has a firm granular structure with some small pores and channels
422 on the surface, whereas LPGS has more surface irregularities and spongy like surface with some
423 degree of fractured particles. (Figure 4 (B)). Accordingly, LPGS appears to have a higher surface
424 area owing to its open interconnected structure. This, however, does not match the $V_m$ and surface
425 area values reported in Table 3. At higher magnification (×1000) it is seen that Starch1500
426 particles have very small pores or channels on the surface of particles shown by arrows. However,
427 the presence of the large potholes on LPGS particles as compared to the packed structure of ST
428 1500, signifies that monolayer formation for ST 1500 is much faster as compared to the fully
429 pregelatinised sample of LPGS powder. It again brings up the concept of ink-bottle water sorption
430 that the packed structure of the partially pregelatinised ST 1500 is able to uptake a similar amount
431 of water compared to the irregular and sponge-like structure of LPGS powder. Moreover, by
432 observing the surface morphology of the LPGS, it is suggested that the compressibility and
433 compactability of the LPGS sample should be relatively higher than the packed structure of ST
434 1500 (this is ongoing research which will be investigated fully in another original research article).
435 Thus, it implies a positive impact on the compressibility and compactability of LPGS as compared
436 to ST 1500, but it does not necessarily influence the volume of water sorbed by the samples and
437 rate of sorption – desorption.
438
439
440

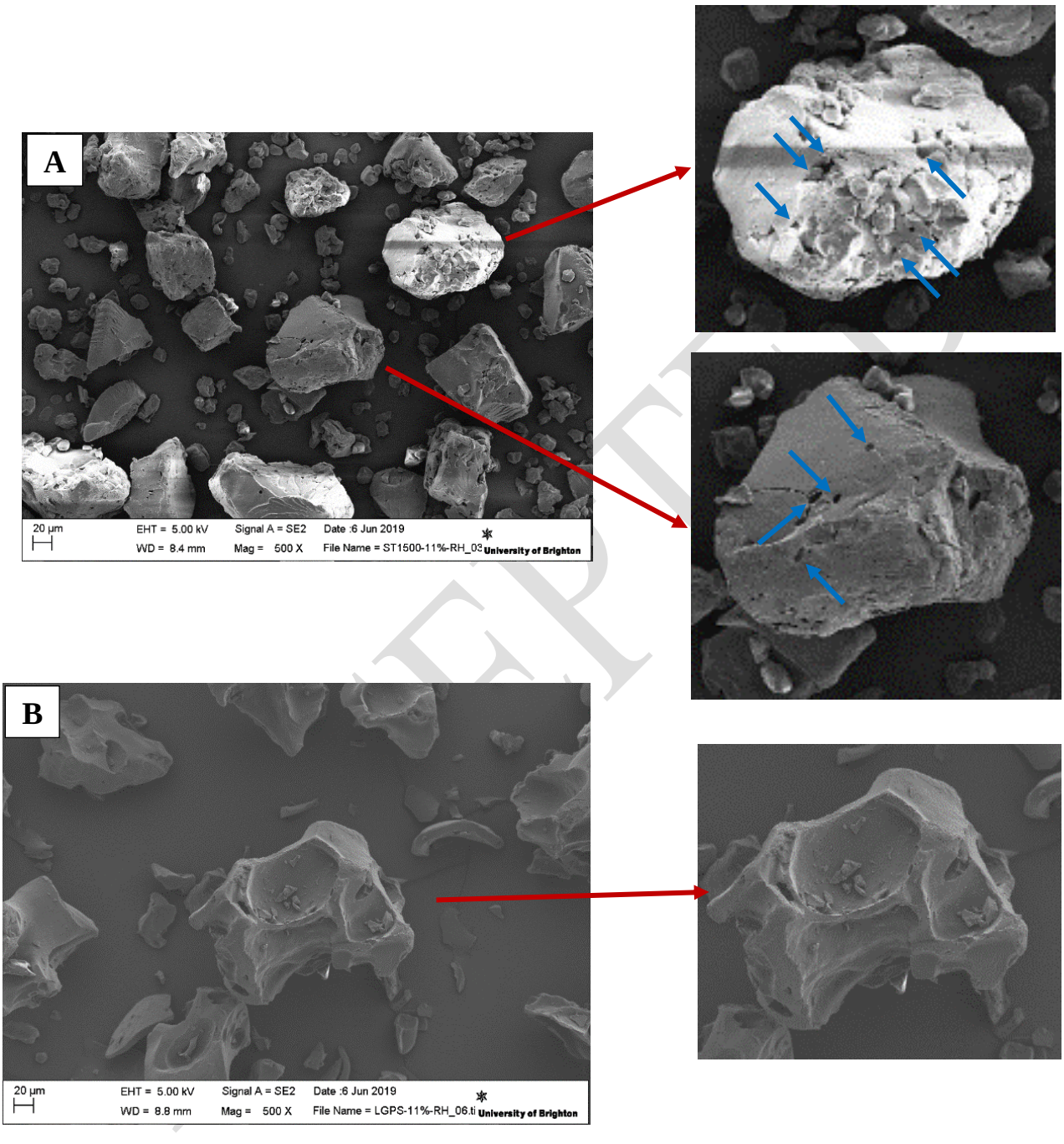


**Figure 4.** SEM images of (A) Starch 1500; (B) LPGS.

FTIR, PXRD and TGA were performed to evaluate whether the changes in the moisture absorption behaviour for partially gelatinised and fully gelatinised starch could be due to their thermal

behaviour and the solid-state of starch-based excipients (crystalline or amorphous). To this end, these experiments were performed, and the results are discussed below.

Figure 5 shows the FT-IR of partially gelatinised starch (Starch 1500) and fully gelatinised starch (Lycatab-PGS). The main absorption bands are at about 3300 (OH groups), 1610, 1350 and 1000 $cm^{-1}$. The absorption bands at 3300 and 1610 $cm^{-1}$ are due to the bound water, while the band at 1350 $cm^{-1}$ is due to the bending vibrational modes of O-C-H, C- C-H, and C- O-H. In the region between 1200 and 900 $cm^{-1}$, several strong absorption peaks are assigned to C-C and C-O stretching modes (Iizuka & Aishima, 1999; Rojas, Uribe, & Zuluaga, 2012). The figure shows that both FT-IR for ST 1500 and Lycatab-PGS are very similar and no significant difference is observed.

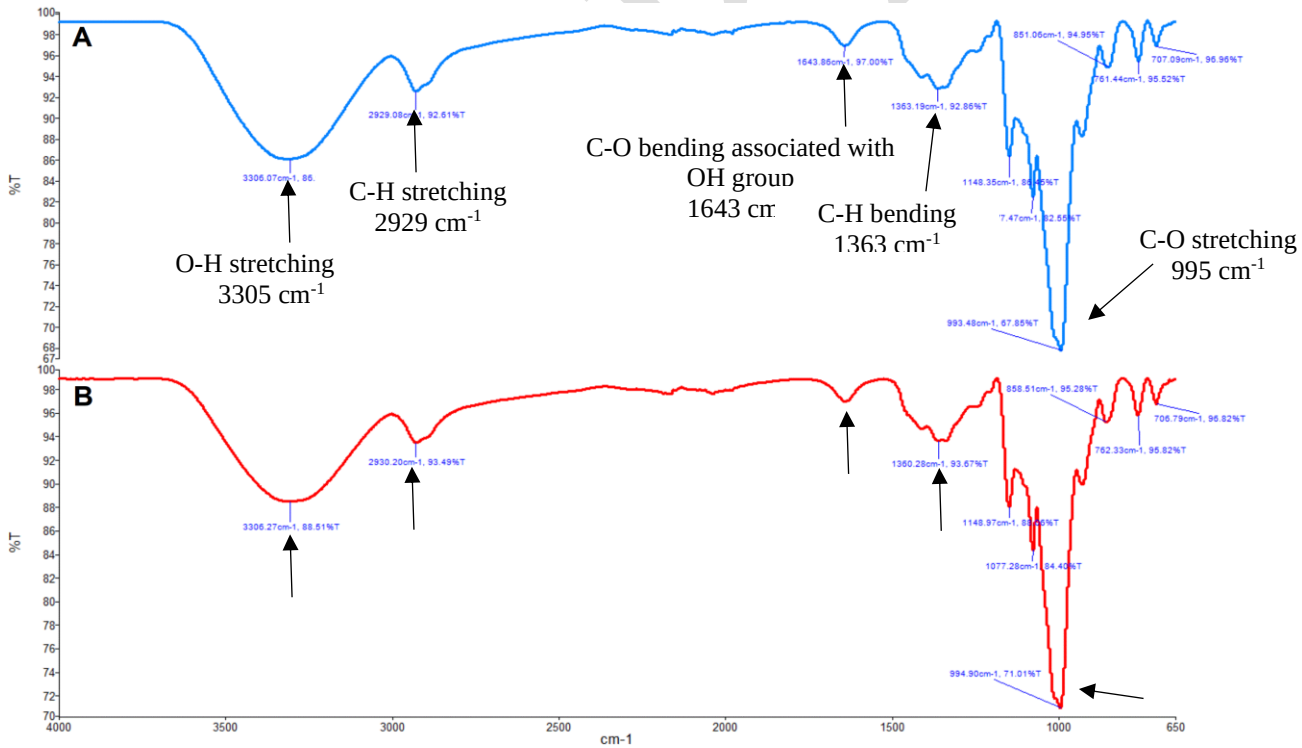


Figure 5. FT-IR of the samples of (A) partially pregelatinised starch (Starch 1500) and (B) fully pregelatinised starch (Lycatab-PGS).

PXRD for these two starch-based excipients is shown in Figure 6. Overall, both excipients show a halo pattern which is an indication of amorphous structure. By careful investigation, Figure 6 shows a peak around 17° for both ST 1500 and Lycatab-PGS. It has been reported that the PXRD of native corn starch (no pregelatinisation), should show more peaks at 2Θ of 15, 17, 20, 23 and 26° (Gao et al., 2014). The absence of these peaks in partially gelatinised and fully gelatinised starches indicates loss of crystalline arrangement due to the rupture of intra and intermolecular hydrogen bonding (Adak & Banerjee, 2016; Lu, Luo, Fu, & Xiao, 2013).

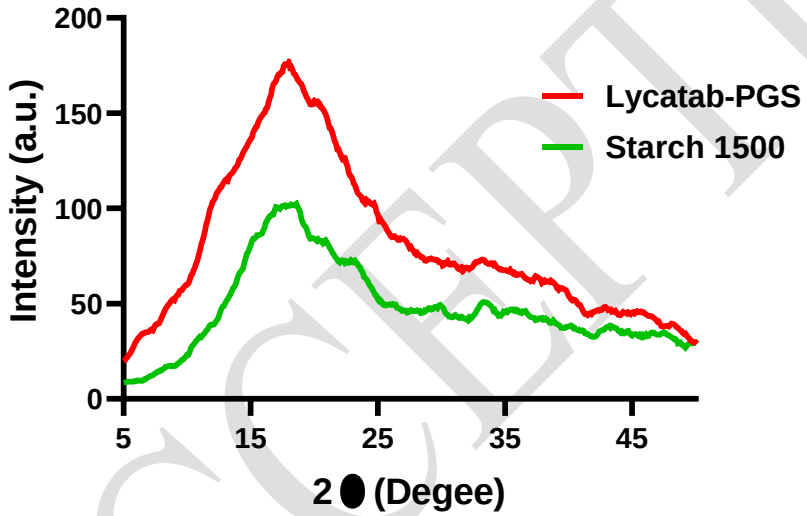


Figure 6. Powder X-Ray Diffractograms of partially gelatinised starch (Starch 1500) and fully gelatinised starch (Lycatab-PGS).

Finally, the TGA curves for Starch 1500 and Lycatab-PGS were shown in Figure 7. As evident from the plots, both starch-based excipients showed a three-stage weight loss between 20 and 495 °C. The first weight loss below 100 °C is due to water evaporation (Gao et al., 2014; Zhang, Xie, Zhao, Liu, & Gao, 2009). The remarkable weight loss between 275-340 °C could be due to

degradation of starch amylose and amylopectin (Beninca et al., 2008). The third weight loss which is less pronounced compared to the second stage could also be due to starch decomposition.

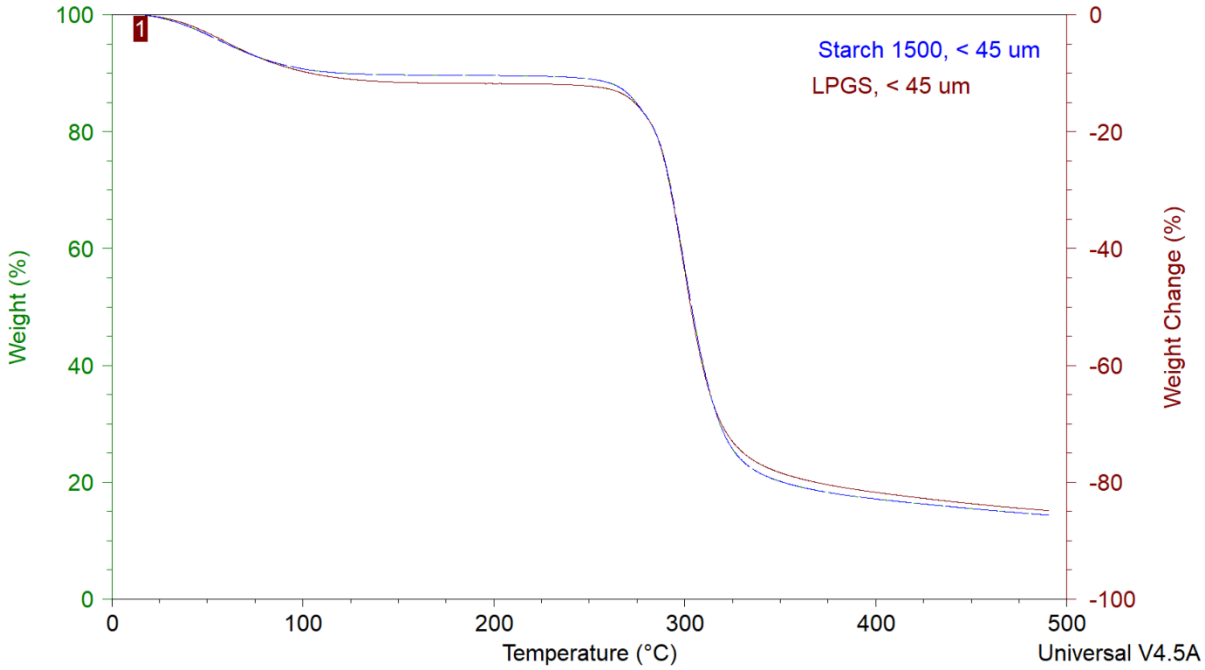


Figure 7. TGA plots of partially gelatinised starch (Starch 1500) and fully gelatinised starch (Lycatab-PGS).

## 3. Conclusion

DVS is a promising method which resembles the dynamic simulation of water sorption in practice. Development of sorption isotherms and study of their characteristic features such as presence and the shape of hysteresis is a critical point to determine the mechanism of sorption-desorption. Starch-based excipients showed type ii (S shape) isotherm according to the IUPAC and Brunauer classification, irrespective of being partially or fully pregelatinised. The appearance of hysteresis reveals that the desorption of water in starch products is an irreversible phenomenon, indicating that some of the sorbed water molecules are either entrapped within the physical structure, which is due to the structural conformation change during sorption cycle at a molecular level. This is attributed to the swelling ability of starch-based excipients when hydrated. It was found that the

particle size difference does not have any influence on the rate of water sorption, even though calculated parameters of Young and Nelson model showed the variables are different for various particle size fractions of starchy excipients. It was concluded that the degree of pregelatinisation influences the rate of moisture sorption. Thus, the higher the pregelatinisation degree, more time is required for the sample to take up (absorb) moisture. The obtained data were fitted into the BET model to calculate the volume of the fraction of the powders adsorbed on the surface ($V_m$). Therefore, it can also infer that by reducing the surface area the volume of the absorbed water will also reduce. The results of this research are of great importance in the utilisation of Starch 1500 as pertains to the development of stable formulations for moisture-sensitive drug molecules.

**Conflict of interest**

All authors declare no conflict of interest.

**Acknowledgement**

Saeid Rajabnezhad would like to thank Colorcon Limited, UK for providing the funding for this PhD study.

References

Adak, S., & Banerjee, R. (2016). A green approach for starch modification: Esterification by lipase and novel imidazolium surfactant. *Carbohydrate Polymers*, *150*, 359–368.

Anderson, R. B. (1946). Modifications of the Brunauer, Emmett and Teller Equation. *Journal of the American Chemical Society*, *68*(4), 686–691.

Beninca, C., Demiate, I. M., Lacerda, L. G., Carvalho Filho, M. A. S., Ionashiro, M., & Schnitzler, E. (2008). Thermal behavior of corn starch granules modified by acid treatment at 30 and

50°C. *Eclética Química*, *33*(3), 13–18.

Blahovec, J., & Yanniotis, S. (2008). GAB Generalized Equation for Sorption Phenomena. *Food and Bioprocess Technology*, *1*(1), 82–90.

Brunaubr, S., & Emmett, P. H. (1935). The use of van der waals adsorption isotherms in determining the surface area of iron synthetic ammonia catalysts. *Journal of the American Chemical Society*, *57*(9), 1754–1755.

Brunauer, S., Deming, L. S., Deming, W. E., & Teller, E. (1940). On a Theory of the van der Waals Adsorption of Gases. *Journal of the American Chemical Society*, *62*(7), 1723–1732.

Brunauer, S., Emmett, P. H., & Teller, E. (1938). Adsorption of Gases in Multimolecular Layers. *Journal of the American Chemical Society*, *60*(2), 309–319.

Bulletin, T., Pregelatinized, P., & Starch, M. (2012). Starch 1500 ® partially pregelatinized maize starch. *Colorcon*, Vol. 1, p. 2. Retrieved from https://www.colorcon.com/products-formulation/all-products/download/57/114/34?method=view

Cundell, T. (2015). The role of water activity in the microbial stability of non-sterile drug products. *European Pharmaceutical Review*, Vol. 20, pp. 58–63.

Delwiche, S. R., Pitt, R. E., & Norris, K. H. (1991). Examination of Starch-Water and Cellulose-Water Interactions With Near Infrared (NIR) Diffuse Reflectance Spectroscopy. *Starch - Stärke*, *43*(11), 415–422.

Gao, Y., Wang, L., Yue, X., Xiong, G., Wu, W., Qiao, Y., & Liao, L. (2014). Physicochemical properties of lipase-catalyzed laurylation of corn starch. *Starch - Stärke*, *66*(5–6), 450–456.

Iizuka, K., & Aishima, T. (1999). Starch Gelation Process Observed by FT-IR/ATR Spectrometry with Multivariate Data Analysis. *Journal of Food Science*, *64*(4), 653–658.

Iglesias, H. A., & Chirife, J. (1995). An alternative to the Guggenheim, Anderson and De Boer model for the mathematical description of moisture sorption isotherms of foods. *Food Research International*, *28*(3), 317–321.

Inglezakis, V. J., Poulopoulos, S. G., & Kazemian, H. (2018). Insights into the S-shaped sorption isotherms and their dimensionless forms. *Microporous and Mesoporous Materials*, *272*, 166–

176.

Kawongolo, J. B. (2013). *Optimization of Processing Technology for Commercial Drying of Bananas ( Matooke )* (Universität Kassel). Retrieved from https://d-nb.info/1051471990/34

Likar, M. D., Taylor, R. J., Fagerness, P. E., Hiyama, Y., & Robins, R. H. (1993). The 3′-Keto–Diol Equilibrium of Trospectomycin Sulfate Bulk Drug and Freeze-Dried Formulation: Solid-State Carbon-13 Cross-Polarization Magic Angle Spinning (CP/MAS) and High-Resolution Carbon-13 Nuclear Magnetic Resonance (NMR) Spectroscopy Studies. *Pharmaceutical Research: An Official Journal of the American Association of Pharmaceutical Scientists*, *10*(1), 75–79.

Lu, X., Luo, Z., Fu, X., & Xiao, Z. (2013). Two-Step Method of Enzymatic Synthesis of Starch Laurate in Ionic Liquids. *Journal of Agricultural and Food Chemistry*, *61*(41), 9882–9891.

Malamataris, S., Goidas, P., & Dimitriou, A. (1991). Moisture sorption and tensile strength of some tableted direct compression excipients. *International Journal of Pharmaceutics*, *68*(1–3), 51–60.

Nokhodchi, A., Ford, J. L., & Rubinstein, M. H. (1997). Studies on the Interaction Between Water and (Hydroxypropyl)Methylcellulose. *Journal of Pharmaceutical Sciences*, *86*(5), 608–615.

Ostrowska-Ligęza, E., Jakubczyk, E., Górska, A., Wirkowska, M., & Bryś, J. (2014). The use of moisture sorption isotherms and glass transition temperature to assess the stability of powdered baby formulas. *Journal of Thermal Analysis and Calorimetry*, *118*(2), 911–918.

Peleg, M. (1988). An Empirical Model for the Description of Moisture Sorption Curves. *Journal of Food Science*, *53*(4), 1216–1217.

Peleg, M. (1993). Assessment of a semi-empirical four parameter general model for sigmoid moisture sorption isotherms. *Journal of Food Process Engineering*, *16*(1), 21–37.

Reutzel-Edens, S. M., Braun, D. E., & Newman, A. W. (2018). Hygroscopicity and Hydrates in Pharmaceutical Solids. In R. Hilfiker & M. von Raumer (Eds.), *Polymorphism in the Pharmaceutical Industry* (pp. 159–188).

Rojas, J., Uribe, Y., & Zuluaga, A. (2012). Powder and compaction characteristics of

pregelatinized starches. *Pharmazie*, *67*(6), 513–517.

Saripella, K. K., Mallipeddi, R., & Neau, S. H. (2014a). Crospovidone Interactions with Water. I. Calorimetric Study of the Effect of Polyplasdone Particle Size on Its Uptake and Distribution of Water. *Journal of Pharmaceutical Sciences*, *103*(2), 669–675.

Saripella, K. K., Mallipeddi, R., & Neau, S. H. (2014b). Crospovidone interactions with water. II. Dynamic vapor sorption analysis of the effect of Polyplasdone particle size on its uptake and distribution of water. *International Journal of Pharmaceutics*, *475*(1–2), 174–180.

Sing, K. S. W. (1985). Reporting physisorption data for gas/solid systems with special reference to the determination of surface area and porosity (Recommendations 1984). *Pure and Applied Chemistry*, *57*(4), 603–619.

Sing, K.S.W. (1994). Physisorption of gases by carbon blacks. *Carbon*, *32*(7), 1311–1317.

Staudt, P. B., Tessaro, I. C., Marczak, L. D. F., Soares, R. D. P., & Cardozo, N. S. M. (2013). A new method for predicting sorption isotherms at different temperatures: Extension to the GAB model. *Journal of Food Engineering*, *118*(3), 247–255.

Young, J. H & Nelson, G. L. (1967a). Research of Hysteresis Between Sorption and Desorption Isotherms of Wheat. *Transactions of the ASAE*, *10*(6), 0756–0761.

Young, J. H & Nelson, G. L. (1967b). Theory of Hysteresis Between Sorption and Desorption Isotherms in Biological Materials. *Transactions of the ASAE*, *10*(2), 0260–0263.

York, P. (1981). Analysis of moisture sorption hysteresis in hard gelatin capsules, maize starch, and maize starch: drug powder mixtures. *Journal of Pharmacy and Pharmacology*, *33*(1), 269–273.

Yu, H., & Li, Y. (2015). State Diagram of Spray Dried Bovine Colostrum Powder. *International Journal of Food Properties*, *18*(3), 480–491.

Zeng, Y., Fan, C., Do, D. D., & Nicholson, D. (2014). Evaporation from an Ink-Bottle Pore: Mechanisms of Adsorption and Desorption. *Industrial & Engineering Chemistry Research*, *53*(40), 15467–15474.

Zhang, L., Xie, W., Zhao, X., Liu, Y., & Gao, W. (2009). Study on the morphology, crystalline

structure and thermal properties of yellow ginger starch acetates with different degrees of substitution. *Thermochimica Acta*, *495*(1–2), 57–62.